Selectivity of Surface Defects for the Activation of Supported Metal Atoms: Acetylene Cyclotrimerization on Pd_1/MgO

Anna Maria Ferrari,[†] Livia Giordano,[‡] Gianfranco Pacchioni,*[,‡] Sthephane Abbet,[§] and Ueli Heiz[||]

Dipartimento di Chimica IFM, Università di Torino, via P. Giuria 5, I-10125 Torino, Italy, Dipartimento di Scienza dei Materiali, Università di Milano-Bicocca and Istituto Nazionale per la Fisica della Materia, via R. Cozzi 53, I-20125 Milano, Italy, Institut de Physique de la Matière Condensée, Université de Lausanne, CH-1015 Lausanne, Switzerland, and Institute of Surface Chemistry and Catalysis, University of Ulm, D-89069 Ulm, Germany

Received: October 10, 2001; In Final Form: November 29, 2001

We report on the results of density functional cluster model calculations on thermodynamical and kinetical aspects of the acetylene cyclotrimerization reaction occurring on single Pd atoms deposited with soft-landing techniques on MgO(100) thin films. The different elementary steps of the reaction as well as the transition states involved have been investigated in detail for Pd atoms adsorbed on different sites of MgO to understand the role of the substrate in this reaction. The analysis of the complete reaction path indicates that only basic defect sites such as neutral and charged oxygen vacancies (F and F^+ centers) located at the MgO terraces can activate supported Pd atoms for this process.

1. Introduction

The reaction of acetylene cyclotrimerization to form benzene, $3C_2H_2 \rightarrow C_6H_6$, has been widely studied on single-crystal surfaces under UHV conditions ($10^{-12}-10^{-8}$ atm) as well as atmospheric pressure ($10^{-1}-1$ atm).[1−4] Pd(111) is the most reactive surface,[5,6] and the reaction proceeds through the formation of a stable C_4H_4 intermediate, formed by the addition of two acetylene molecules:[7]

$$Pd + 2C_2H_2 \rightarrow Pd(C_2H_2)_2 \rightarrow Pd(C_4H_4) \quad (1)$$

The C_4H_4 intermediate has been characterized experimentally[8−10] and theoretically.[11] Once the C_4H_4 intermediate is formed, it can add a third acetylene molecule to form benzene:[1,2]

$$Pd(C_4H_4) + C_2H_2 \rightarrow Pd(C_4H_4)(C_2H_2) \rightarrow Pd(C_6H_6) \quad (2)$$

At low coverage and on flat Pd(111) surfaces the formed benzene molecule is adsorbed parallel to the surface and desorbs at about 500 K.[1,2] The formation of benzene on Pd particles a few nanometers in size is very similar to the analogous low-index single-crystal results, with desorption of benzene at 530 K.[3]

The acetylene cyclotrimerization has been recently studied on small MgO-supported Pd_n ($1 \leq n \leq 30$) clusters. The Pd cluster ions are produced by a laser evaporation source, are then guided by ion optics through differentially pumped vacuum chambers, and are size-selected by a quadrupole mass spectrometer.[12−14] The monodispersed clusters have been deposited with low kinetic energy onto a MgO thin film grown on a Mo(100) surface at 90 K to preserve their nuclearity and prevent the aggregation. The cluster-assembled materials obtained in this way exhibit peculiar activity and selectivity in the polymerization of acetylene to form benzene and aliphatic hydrocarbons.[15] Surprisingly, even a single supported Pd atom has been found to be active in the benzene formation at 300 K.[13,16] On small Pd clusters a second desorption peak is observed at 430 K, suggesting that a different mechanism takes place on single Pd atoms or nanoclusters. The peculiar activity of Pd atoms has been rationalized by means of quantum chemical calculations.[13,16] The activation of the acetylene molecules is easily monitored, for instance, by the deviation from linearity of the HCC angle due to a change in hybridization of the C atom from sp to sp^2 or by the elongation of the C−C distance, d(C−C), as a consequence of charge transfer from the metal 4d orbitals to the empty π^* orbital of acetylene. It was shown[13,16] that only in the presence of surface defects a Pd atom becomes an active catalyst for the reaction; in fact, although an isolated Pd atom forms the intermediate C_4H_4, it cannot adsorb the third acetylene molecule, an essential step for the process. The change in the electronic structure of supported Pd is indeed connected to the donor ability of the support, which does not simply act as an inert substrate. The oxide surface acts in a similar way as a ligand in coordination chemistry and provides an additional source of electron density which increases the capability of the Pd atom to back-donate charge to the adsorbed hydrocarbons. In this respect it is remarkable that on transition metal complexes the acetylene trimerization reaction follows a mechanism very similar to that on heterogeneous supported catalysts:[17] the reaction proceeds through the oxidative coupling of two acetylene ligands to form the metal−C_4H_4 (cycle) intermediate followed by coordination of a third acetylene molecule; the benzene formation occurs via an intramolecular metal-mediated [4 + 2] cycloaddition of the metal−cycle with the coordinated alkyne.

Previous studies[13,14,16] have clearly shown the crucial role of the defect sites present on the oxide surface for the stabilization and the activation of the supported Pd atoms. This opens new important questions about nature, structure, and number of point defects which are active in promoting the reaction. An important

* Corresponding author. E-mail: gianfranco.pacchioni@mater.unimib.it
[†] Università di Torino.
[‡] Università di Milano-Bicocca and Istituto Nazionale per la Fisica della Materia.
[§] Université de Lausanne.
[||] University of Ulm.

10.1021/jp013766+ CCC: $22.00
Published on Web 03/05/2002

consideration concerns therefore the actual localization of the Pd atoms on the MgO thin film. At the moment, this can only be inferred indirectly from comparison of experimental data and theoretical models, since there is no single spectroscopy which is sensitive enough to detect and identify the comparably small number of these centers. In a recent investigation the CO molecule was used as a probe for the characterization of the sites where the Pd atoms are adsorbed.[18] The adsorption properties of the supported Pd−CO complexes were found to be hardly reconcilable with the picture of Pd atoms bound to the MgO oxide anions, located either on terraces or on low-coordinated sites. Much more consistent with the observation is the hypothesis that the Pd atoms are bound to the oxygen vacancies or F centers.[18]

The scope of this work is to verify if the idea of Pd atoms stabilized at F centers is consistent with the energetics and the mechanism of the trimerization reaction. This implies the computation of all the reaction steps for a number of defect centers where the Pd atoms can be bound. In fact, the MgO defects may affect the activation barriers as well as the thermodynamic stability of the intermediates involved in the reaction. So far, the analysis of the influence of the substrate on the energetics of the reaction has been done considering only the stability of the $Pd(C_4H_4)(C_2H_2)$ complex,[16] see reaction 2, as a crucial step in the entire process. Therefore a theoretical analysis of the complete reaction path, from the coordination of the first acetylene molecule to benzene formation and desorption, is necessary to give a more definitive answer on the kind of defect involved in the enhanced Pd activity.

Density functional theory calculations have been performed with the help of model clusters. To allow a better comparison with experimental evidences some specific steps of the process have been also investigated using simple models of the Pd-(111) surface. The results show that only the models of Pd atoms stabilized at F centers are consistent with the proposed reaction mechanism and with the observed benzene desorption temperature.

2. Computational Techniques and Models

We have used an embedded cluster approach[19] to model reactions 1 and 2 occurring on Pd atoms adsorbed on different sites of the MgO surface: terraces; low-coordinated sites (edges or corners); oxygen vacancies (5-, 4-, or 3-coordinated). These sites have been represented by the following clusters: O_9Mg_5 for terrace, $O_{10}Mg_4$ for edge, and O_7Mg_3 for corner, Figure 1. Neutral, F_s, and positively charged, F_s^+, oxygen vacancies have been modeled by removing the oxygen atom from the center of the cluster. We also used a planar Pd_6 cluster to describe the Pd(111) surface, Figure 1. This small model does not provide a realistic description of the surface but is useful to outline the main differences between the reaction occurring on Pd(111) and on Pd_1/MgO. The same model has been used in studying the cyclotrimerization reaction on Pd(111).[11]

The MgO clusters have been embedded in effective core potentials (ECP) and a large array of point charges (PC) to represent the Madelung potential in the cluster region.[20] The reliability of this approach in describing the MgO surface has been widely proven, also in comparison with other embedding schemes and periodic calculations.[21,22] The positions of the adsorbed molecules, of Pd, and of its first neighbors on the MgO surface have been optimized. The transition state search has been performed using the Berny algorithm; in selected cases we have confirmed the nature of the optimized geometries (as minima or transition structures) and the association of the transition state vector with the expected vibrational motion, by a vibrational frequency analysis. The reaction mechanism and all the structures have been investigated imposing a symmetry plane (C_s symmetry).

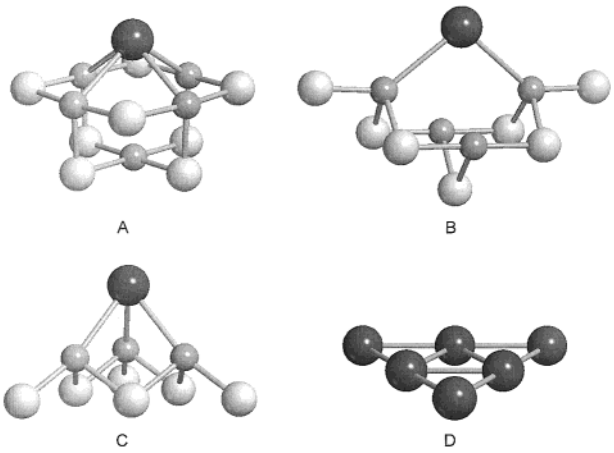

Figure 1. Cluster models of a Pd atom adsorbed on (A) an oxygen vacancy at a MgO terrace, F_{5C}, (B) an oxygen vacancy at a MgO edge, F_{4C}, and (C) an oxygen vacancy at a MgO corner, F_{3C}, and (D) a Pd_6 cluster model of the Pd(111) surface: small gray spheres, Mg; large white spheres, O; large dark spheres, Pd.

Gaussian-type atomic orbital basis sets were employed to construct the Kohn−Sham orbitals. The 6-31G basis set has been used for O and Mg.[23] In the F_s and F_s^+ cases, where one or two electrons, respectively, are trapped in the vacancy, a diffuse 6-31+G basis set has been employed on the Mg atoms nearest the vacancy to describe the electron localization in the cavity.[24] A 18-electron ECP where the $4s^24p^64d^{10}$ electrons are explicitly treated in the valence and a double-ζ plus polarization basis have been used for Pd (LanL2DZ),[25] while C and H have been treated with a 6-311G(p,d) basis.

The calculations have been performed at the DF level. Despite the great advances in the development of new exchange-correlation functionals, the question of which functional provides the best chemical accuracy is still under discussion. In particular, the choice of the functional has been shown[26,27] to be crucial for the description of the transition metal−oxide interface. An extreme case is that of Cu adsorption on MgO: the reported adsorption energies range from a practically unbound Cu atom at the Hartree−Fock (HF) level to a moderate adsorption, 0.35−0.90 eV, at gradient corrected DF level, to strong adsorption, about 1.5 eV, using the local density approximation, LDA. Recently, Ranney et al.[28] have extrapolated the adhesion energy of a Cu atom on MgO from their microcalometric measures of the heat of adsorption and have found a value of 0.7 eV. The comparison of this value with the computed adsorption energies of ref 26 indicates that, among the currently used approximation of the exchange-correlation functionals, the pure DF ones seem to provide the best answer, while hybrid functionals (which contain a HF exchange part), slightly underestimate the adsorption energy. In particular the gradient-corrected Becke−Perdew (BP) functional, where the Becke's exchange[29] is combined with the Perdew's correlation functional,[30] yields a value for the Cu adsorption energy, 0.8 eV, close to the experimental estimate.[28] A considerably lower value, 0.35 eV, is computed with the B3LYP functional built up by the Becke's three parameter hybrid exchange functional[31] in combination with the correlation functional of Lee, Yang, and Parr.[32] We have chosen to perform all calculations using the BP functional and to compare the results with B3LYP calculations for selected cases.

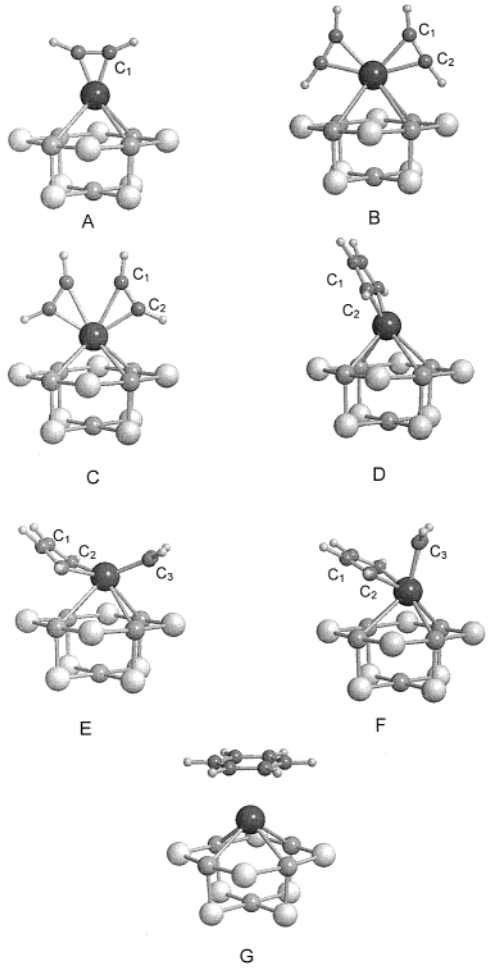

Figure 2. Optimal structures of the different intermediates in the acetylene trimerization reaction occurring on a Pd atom supported on a neutral oxygen vacancy at a terrace site, Pd/F_{5c}: (A) coordination of an acetylene molecule; (B) coordination of a second acetylene molecule; (C) transition state for the C_4H_4 intermediate formation; (D) C_4H_4 intermediate; (E) coordination of a third acetylene molecule; (F) transition state for benzene formation; (G) bonding of the benzene molecule. See Figure 1 for the definition of cluster atoms.

The results presented in this work, aimed at the determination of the energy barriers and the reaction mechanisms, have not been corrected for the basis set superposition error (BSSE).[33] From our previous work, performed with an equivalent computational scheme, we can expect a BSSE of about 0.1−0.2 eV for the Pd−acetylene bonding.[16]

All calculations have been performed with the GAUSSIAN98[34] package; in some cases an analysis of the wave function has been performed at the HF level using the constrained space orbital variation, CSOV,[35] method which allows one to decompose the interaction energy into the sum of single contributions. Recently it has been shown that similar qualitative conclusions can be obtained from CSOV analyses performed at HF or DFT levels.[36] In this case the calculations have been performed using the HONDO[37] program package. Only qualitative aspects of the CSOV will be discussed.

3. Results

According to recent homogeneous catalysis studies[17] and surface science investigations[1,3,9,11,13] the process $3C_2H_2 \rightarrow C_6H_6$ takes place via the following steps (as sketched in Figure 2 for the case of a Pd atom supported on a terrace oxygen vacancy center):

(i) coordination and activation of a single acetylene molecule, Figure 2A;

(ii) coordination of a second acetylene molecule, Figure 2B;

(iii) formation of an activated complex, Figure 2C, and of the C_4H_4 intermediate, Figure 2D;

(iv) coordination of a third acetylene molecule, Figure 2E;

(v) formation of a second activated complex, Figure 2F, and of adsorbed benzene, Figure 2G, followed by benzene desorption.

In the following we analyze in detail each of these steps for three groups of MgO surface defects namely O_{nC}^{2-} sites, neutral F_{nC} centers, and charged F_{nC}^{+} centers, where *n*C indicates the coordination number of the site, 3C (corner), 4C (edge), or 5C (terrace).

3.1. Coordination and Activation of One Acetylene Molecule. We start with the bonding of acetylene to Pd atoms located at oxide sites, Pd/O_{5C}^{2-}, Pd/O_{4C}^{2-}, and Pd/O_{3C}^{2-}, respectively, Table 1. At these sites the Pd atom is bound with adsorption energies of about 1, 1.4, and 1.5 eV, respectively (B3LYP results from ref 18). Upon adsorption, the C_2H_2 molecule becomes considerably activated as monitored by the distorted angle, $\angle(H-C-C) \sim 155°$, and by the elongation of the C−C distance with respect to the gas-phase value, Table 1. The $Pd-C_2H_2$ interaction is rather strong: the computed binding energies at BP level are 1.94 eV for Pd/O_{5C}^{2-}, 1.81 eV for Pd/O_{4C}^{2-}, and 2.01 eV for Pd/O_{3C}^{2-}. The B3LYP functional gives slightly weaker interactions (about 0.3 eV smaller) and essentially the same geometrical structure, Table 1. Both geometry and binding energy show only minor differences with respect to unsupported Pd atoms, Table 1.

We consider now the case of Pd atoms supported at the F_S centers. Here the bonding of Pd is much stronger and goes from 3.4 to 3.7 eV,[18,38,39] depending on the coordination of the F center. These defect sites are characterized by the presence of two electrons trapped in the cavity, and they present an even more basic character than the O^{2-} centers. However, when the Pd atom is adsorbed on a F_S center, the binding of the acetylene molecule decreases considerably. The molecule is bound by 0.07−0.3 eV at the BP level while using a B3LYP functional only the bonding with the Pd/F_{5C} complex survives, Table 1. The Pd/O_{nC}^{2-} bond has been described as prevalently covalent with only moderate charge transfer and polarization toward the metal atom.[40,41] On the contrary, the strong Pd/F_{nC} interaction originates mainly from the electron transfer from the cavity to the adatom.[12,13,18] Therefore, the two electrons in the vacancy are largely delocalized over the 5s orbital of Pd, thus increasing its density.[42] A quantitative estimate of the charge transfer is not trivial, as the Mulliken analysis is strongly dependent on the basis set used. In fact, in the literature values between 0.2 and 0.8 electrons have been reported;[39,43] our calculations indicate a charge transfer close to one electron. These oscillations are not surprising as a more diffuse representation of the 5s orbital results in a strong increase in the charge transfer. Since atomic charges are not physical observables, these differences do not have any special meaning. The CSOV decomposition of the wave function shows that the augmented electron density on Pd leads to a stronger Pauli repulsion with acetylene. To reduce the Pauli repulsion the acetylene molecule binds to Pd/F_{nC} at a distance which is 0.10−0.15 Å longer than on the corresponding Pd/O_{nC}^{2-} complex, Table 1. The basic character of the F_{nC} sites is manifested by the large π back-donation from the metal to C_2H_2; as a consequence, the molecule is highly distorted, Table 1, despite the weak adsorption energy.

TABLE 1: Adsorption Properties of One C_2H_2 Molecule on the S/Pd Complex (S = O^{2-}, F_S, F_S^+)

C_2H_2	Pd	Pd/$O^{2-}{}_{5C}$	Pd/$O^{2-}{}_{4C}$	Pd/$O^{2-}{}_{3C}$	Pd/F_{5C}	Pd/F_{4C}	Pd/F_{3C}	Pd/$F^+{}_{5C}$	Pd/$F^+{}_{4C}$	Pd/$F^+{}_{3C}$
$d(C_1–C_1)$,[a] Å	1.269	1.267	1.262	1.269	1.261	1.233	1.244	1.247	1.240	1.253
$d(C_1–Pd)$, Å	2.048	2.060	2.076	2.057	2.040	2.328	2.241	2.170	2.230	1.079
$\angle(H–C_1–C_1)$, deg	154.9	154.5	156.6	153.7	156.4	168.5	163.8	161.5	164.5	159.6
BE_{BP},[b] eV	1.84	1.89	1.83	2.00	0.36	0.08	0.13	0.70	0.66	0.96
BE_{B3LYP},[b] eV	1.28	1.50	1.46	1.66	0.09	unbound	unbound	0.44	0.45	0.44

[a] Free C_2H_2 at BP level: $d(C–C)$ = 1.209 Å; $d(C–H)$ = 1.071 Å. [b] Binding energy, BE, computed as BE = $E[S/Pd/(C_2H_2)] - E[C_2H_2] - E[S/Pd]$.

TABLE 2: Adsorption Properties of Two C_2H_2 Molecules on the S/Pd Complex (S = O^{2-}, F_S, F_S^+)

		Pd	Pd/$O^{2-}{}_{5C}$	Pd/$O^{2-}{}_{4C}$	Pd/$O^{2-}{}_{3C}$	Pd/F_{5C}	Pd/F_{4C}	Pd/F_{3C}	Pd/$F^+{}_{5C}$	Pd/$F^+{}_{4C}$	Pd/$F^+{}_{3C}$
$(C_2H_2)(C_2H_2)$	$d(C_1–C_2)$, Å	1.250	1.259	1.270	1.266	1.258	1.277	1.321	1.247	1.260	1.282
	$d(C_1–Pd)$, Å	2.180	2.149	2.098	2.127	2.206	2.119	2.164	2.245	2.172	2.093
	$d(C_2–Pd)$, Å	2.132	2.174	2.204	2.124	2.206	2.215	2.074	2.234	2.244	2.001
	$\angle(H–C_1–C_2)$, deg	163.0	154.4	150.9	154.0	153.6	147.9	132.9	160.2	156.6	145.8
	$\angle(H–C_2–C_1)$, deg	157.1	171.2	150.8	153.1	173.2	145.1	135.9	173.4	147.9	149.3
	BE_{BP},[a] eV	1.09	0.94	0.87	0.63	0.62	1.10	2.06	0.53 (0.31)[b]	0.79	1.46
$(C_2H_2)(C_2H_2)^‡$	$d(C–C)$, Å				1.322	1.286	1.297	1.315	1.297	1.297	1.305
	$d(C_1–Pd)$, Å				2.274	2.470	2.261	2.189	2.368	2.313	2.308
	$d(C_2–Pd)$, Å				2.093	2.119	2.138	2.173	2.099	2.114	2.126
	$\angle(H–C_1–C_2)$, deg				129.9	141.7	140.7	136.9	136.3	137.5	137.6
	$\angle(H–C_2–C_1)$, deg				125.4	146.0	134.8	127.2	137.1	132.2	128.1
	$\Delta E_{BP}^‡$,[c] eV				1.73	0.48	0.30	1.39	1.07 (1.35)[b]	0.70	1.42
C_4H_4	$d(C_1–C_1)$, Å	1.464	1.462	1.461	1.462	1.460	1.491	1.497	1.460	1.470	1.480
	$d(C_2–C_1)$, Å	1.350	1.354	1.355	1.357	1.360	1.360	1.370	1.352	1.355	1.366
	$d(C_2–Pd)$, Å	1.995	2.007	2.014	2.006	2.042	2.188	2.204	2.043	2.134	2.105
	ΔE_{BP},[d] eV	0.93	0.83	0.88	1.32	0.82	1.25	0.50	0.87 (0.63)[b]	1.26	1.07

[a] Binding energy, BE, computed as BE = $E[S/Pd/(C_2H_2)(C_2H_2)] - E[C_2H_2] - E[S/Pd/(C_2H_2)]$. [b] DFT−B3LYP results. [c] $\Delta E^‡ = E[S/Pd/(C_2H_2)(C_2H_2)^‡] - E[S/Pd/(C_2H_2)(C_2H_2)]$. [d] $\Delta E = -E[S/Pd(C_4H_4)] - E[S/Pd/(C_2H_2)(C_2H_2)]$.

The weak Pd−C_2H_2 bonding is a direct manifestation of the so-called bond-order conservation theory;[44] in an A−B−C system the increase of the strength of the A−B bond occurs at the expenses of the B−C interaction and vice versa. The strong Pd/F_{nC} bond results in a weak Pd−C_2H_2 interaction. The same effect has been found for CO on MgO supported Pd atoms.[18]

We now consider the paramagnetic F_{nC}^+ centers. On these sites Pd is bound by about 2.1−2.4 eV.[18] These sites are characterized by only one electron trapped in the cavity; therefore, less charge is delocalized on the 5s Pd orbital and the Pauli repulsion toward the acetylene molecule decreases. As a result, on Pd/F_{nC}^+ centers the acetylene is moderately bound at both BP (0.96−0.66 eV) and B3LYP (0.44 eV) levels, Table 1. This stronger interaction does not correspond to a larger activation compared to the neutral F centers as shown by the ∠H−C−C angle, 162°, and by the C−C bond which is about 0.03 Å longer, Table 1. The smaller electronic charge in the cavity leads to a reduced Pd → C_2H_2 back-donation; furthermore, the polarization due to the positive charge of the F_s^+ center and the σ donation from C_2H_2 to Pd play a nonnegligible role in the interaction.

To summarize this section, we have found a strong interaction between the acetylene molecule and the Pd/O_{nC}^{2-} centers while on the Pd/F_{nC} centers the Pauli repulsion leads to a dramatic reduction of the bond strength. On the low-coordinated F_{4C} and F_{3C} centers the Pd/C_2H_2 complex is virtually unbound. The behavior is intermediate in the case of the F_{nC}^+ centers which are able to bind and activate the acetylene molecule irrespective of the coordination of the defect site. We conclude that most of the MgO surface sites considered can in principle be involved in the adsorption and activation of acetylene (the exception are the F_{4C} and F_{3C} sites), although the energetics of the adsorption process varies dramatically from site to site.

3.2. Coordination of a Second Acetylene Molecule. On Pd/O_{nC}^{2-} complexes the coordination of a second alkyne molecule occurs with less energy release than for the first one; in fact the binding energies vary from 0.63 eV for Pd/O_{3C}^{2-}, to 0.87 eV for Pd/O_{4C}^{2-}, and to 0.94 eV for Pd/O_{5C}^{2-}, respectively, Table 2. When an acetylene molecule is already adsorbed on the Pd/F_S surface complex, part of the Pd 5s electron density has been back-donated to acetylene thus reducing the Pauli repulsion toward an incoming molecule. As a result, the second acetylene is strongly bound and activated on Pd/F_{5C} centers (Table 2 and Figure 2). This effect is present but more pronounced on the F_S (the subscript S indicates generically an F center at the surface of MgO) sites at edges and corners, where the adsorption energies of the second acetylene are 1.1 and 2.1 eV, respectively. Notice however that since the first molecule is virtually unbound on these sites (the binding at the BP level is of the same order of the expected BSSE), the bonding with a second acetylene molecule is purely hypothetical because of the very low probability to bind simultaneously two molecules on the same site.

On Pd/F_S^+ the second acetylene molecule is bound on all sites and the strength of the interaction as well as the degree of activation of the molecule follows the trend corner > edge > terrace, Table 2. This is related to the enhanced propensity of the Pd atoms to back-donate charge to the acetylene molecules when the coordination of the defect site is lower.

3.3. C_4H_4 Intermediate Formation. So far the processes considered (acetylene adsorption) are nonactivated. The oxidative coupling of acetylene to form C_4H_4 implies to overcome the first activation barrier for the process. The formation of the C_4H_4 intermediate is a strongly exothermic process since it involves the creation of new σ bonds (C−C and Pd−C) at the expense of π interactions. The geometrical structures of the corresponding transition states are quite different from the reactants, Table 2. Particularly noteworthy are the $C_1–C_1$ distances in Pd(C_4H_4) which are considerably shorter than in Pd(C_2H_2)(C_2H_2) and the elongated "intramolecular" $C_1–C_2$ distances indicating the loss of any remaining C−C triple bond character, Figure 2 and Table 2.[45] Moderately high transition

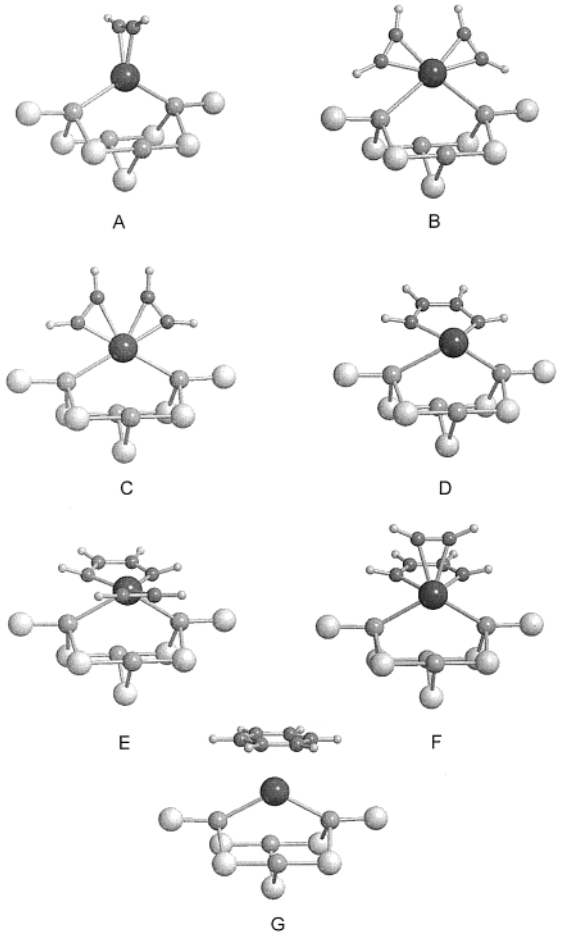

Figure 3. Optimal structures of the different intermediates in the acetylene trimerization reaction occurring on a Pd atom supported on a charged oxygen vacancy at an edge site, Pd/F_{4C}^{+}: (A) coordination of an acetylene molecule; (B) coordination of a second acetylene molecule; (C) transition state for the C_4H_4 intermediate formation; (D) C_4H_4 intermediate; (E) coordination of a third acetylene molecule; (F) transition state for benzene formation; (G) bonding of the benzene molecule. See Figure 1 for the definition of cluster atoms.

barriers have been computed for Pd/F_{nC} and Pd/F_{nC}^{+}, Table 2 and Figures 6−8. The barriers are 0.3−0.7 eV for the F_{5c} and F_{5c}^{+} centers. These barriers are consistent with a low-temperature reaction (below RT (room temperature)). Considerably higher values, >1.4 eV, are found for Pd atoms sitting on low-coordinated O vacancies (with the exception of the neutral F_{4C} defect) or O_{3C} anions (despite several attempts we were unable to locate the transition state for the O_{5C} and O_{4C} sites). Barriers of about 0.5 eV are close to those reported for the CpCo complex.[17] When the Pd atom is supported on the three coordinated sites, Pd/F_{3C}, Pd/F_{3C}^{+}, and Pd/O_{3C}^{2-}, the high barrier has a similar origin: a reduced sterical hindrance from the substrate allows the two alkyne molecules (reactants) to adsorb on the opposite side of Pd, giving a particularly stable structure, Table 2 and Figure 6. Because of this stable starting point, the cost of approaching the two molecules to form the intermediate increases, giving considerable high barriers, Table 2.

To summarize, the barriers computed for the first activated step in the trimerization reaction are quite low for Pd atoms sitting on F_{5C}, F_{4C}, and F_{5C}^{+} sites (0.3−0.7 eV); these barriers are consistent with benzene formation below RT. On all the other sites considered, the barriers are higher than 1.4 eV, indicating that temperatures well above RT are needed for the reaction.

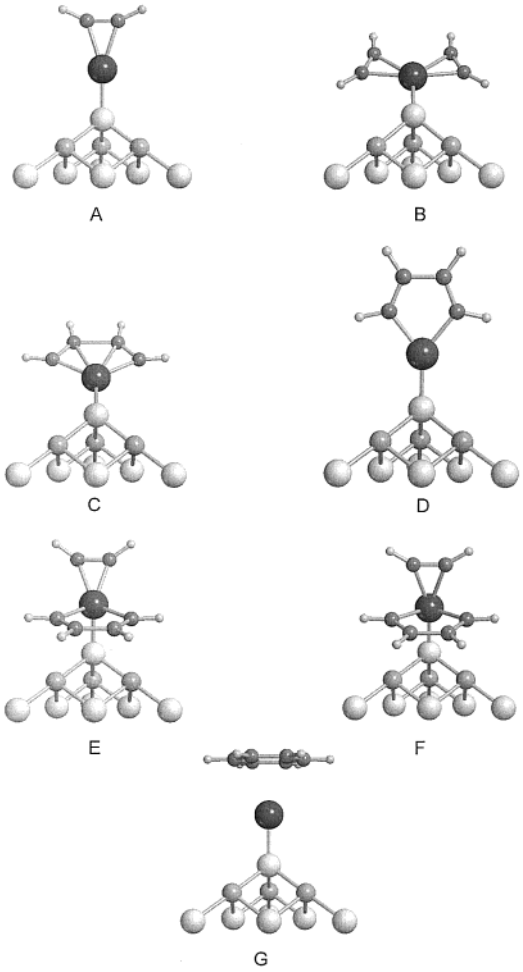

Figure 4. Optimal structures of the different intermediates in the acetylene trimerization reaction occurring on a Pd atom supported on a oxygen ion at a corner site, Pd/O_{3C}^{2-}: (A) coordination of an acetylene molecule; (B) coordination of a second acetylene molecule; (C) transition state for the C_4H_4 intermediate formation; (D) C_4H_4 intermediate; (E) coordination of a third acetylene molecule; (F) transition state for benzene formation; (G) bonding of the benzene molecule. See Figure 1 for the definition of cluster atoms.

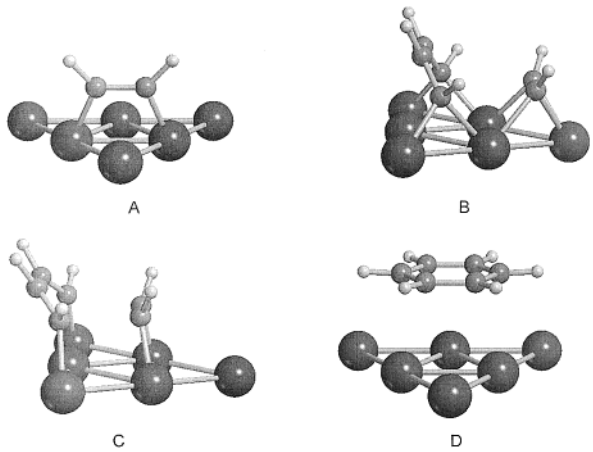

Figure 5. Optimal structures of intermediates in the acetylene trimerization reaction occurring on a Pd(111) surface as represented by a Pd_6 cluster: (A) coordination of an acetylene molecule; (B) C_4H_4 intermediate and coordination of a third acetylene molecule; (C) transition state for benzene formation; (D) bonding of the benzene molecule.

3.4. Coordination of a Third Acetylene Molecule. The following step, $C_4H_4 + C_2H_2 \rightarrow C_6H_6$, requires the capability of the metal center to coordinate and activate a third acetylene

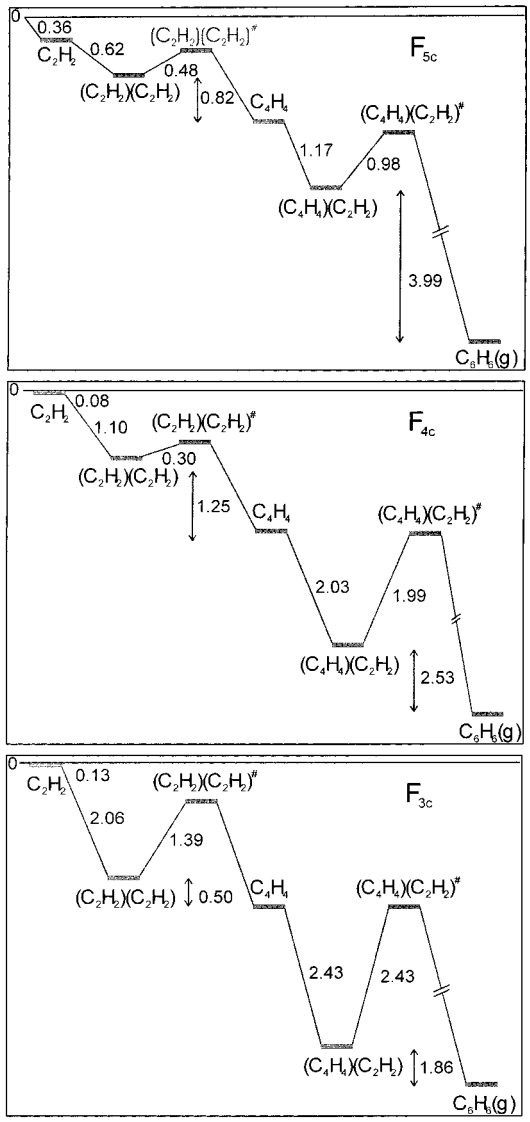

Figure 6. Reaction path for acetylene cyclization on Pd supported on a neutral oxygen vacancy at terrace (F_{5C}, top), edge (F_{4C}, center), and corner (F_{3C}, bottom) sites of the MgO surface. Energies (at the BP level) are in electronvolts.

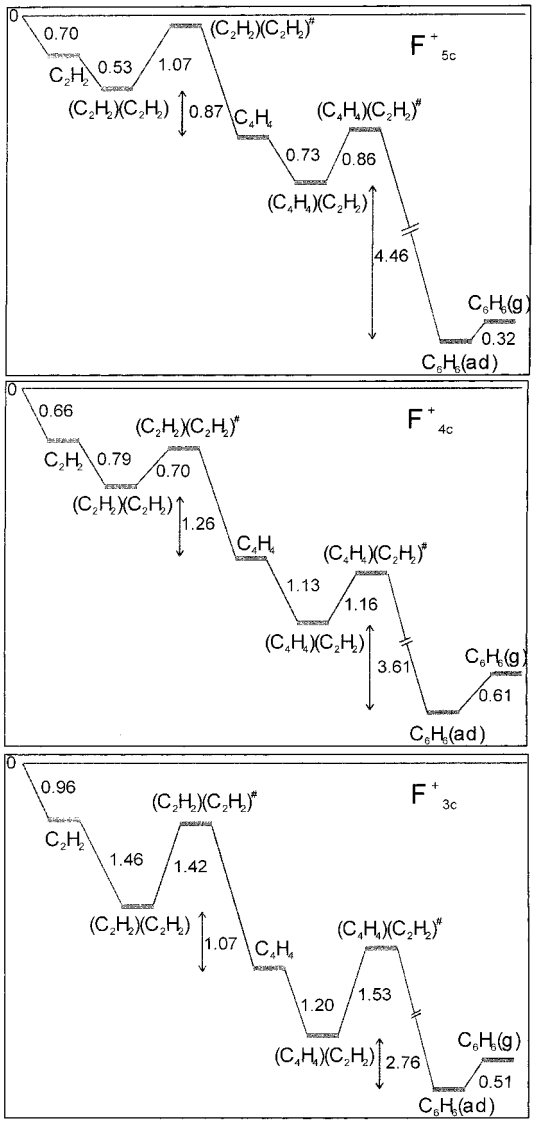

Figure 7. Reaction path for acetylene cyclization on Pd supported on a charged oxygen vacancy at terrace (F_{5C}^+, top), edge (F_{4C}^+, center), and corner (F_{3C}^+, bottom) sites of the MgO surface. Energies (at the BP level) are in electronvolts.

molecule. This is a key step also in the case of transition metal complexes.[17] On a free, unsupported, $Pd(C_4H_4)$ complex the third C_2H_2 molecule is weakly bound (by 0.30 and 0.24 eV at the BP and B3LYP levels, respectively), without an appreciable activation of the molecule, $d(C-C) = 1.216$ Å and $\angle HCC = 177°$, Table 3.[13] Also the oxide sites, O_{nC}^{2-}, are not basic enough to allow the coordination of the third acetylene molecule to Pd. Any attempt to coordinate the molecule at these site was either unsuccessful or gave metastable products. On O_{nC}^{2-} we found a $Pd(C_4H_4)(C_2H_2)$ complex similar to that reported in ref 16 by distorting the C_4H_4 intermediate from its most favored arrangement (almost perpendicular to the surface, Figure 4D) to a tilted configuration almost parallel to the surface. In this structure the $Pd-C_4H_4$ bond is weakened and more electron density is available to bind the third acetylene molecule. However, at the BP level this process is endothermic by 0.7, 0.6, and 1.0 eV for O_{3C}^{2-}, O_{4C}^{2-}, and O_{5C}^{2-}, respectively, and results in unstable products with respect to the dissociation into $Pd(C_4H_4) + C_2H_2$ fragments. At the B3LYP level the third molecule spontaneously dissociates during the geometry optimization. *Thus, Pd atoms bound at regular or low-coordinated O_{nC}^{2-} sites cannot act as catalysts in the trimerization reaction*. On the contrary, the F_{nC} and F_{nC}^+ centers are very strong basic sites; the electrons trapped in the cavity constitute a relevant source of electron density which allows the coordination of a third acetylene molecule. Notice that, upon adsorption, while the geometrical structure of the (C_4H_4) intermediate is actually unvaried, the acetylene molecule shows a considerable distortion ($d(C-C) = 1.26-1.31$ Å and $\angle HCC = 135-157°$, Table 3). The interaction energy of the third acetylene molecule with the supported $Pd(C_4H_4)$ complex follows the usual trend corner > edge > terrace.[16] In general, the values of the binding energy are slightly lower at the F_{nC}^+ centers probably because of the reduced electron density at the vacancy site and of the positive electrostatic potential which disfavor the flow of charge from the substrate to the admolecule.

3.5. Benzene Formation and Desorption. Benzene formation occurs via an intramolecular, metal-mediated [4 + 2] cycloaddition between the $Pd(C_4H_4)$ intermediate and the coordinated acetylene (Figures 2−4). Alternatively, an insertion of the alkyne in the metal−carbon σ bond to form a $Pd-C_6H_6$ metallopentacycle followed by reductive elimination to release benzene is also conceivable. However, two considerations guided our investigation. First of all, homogeneous metal catalysts such as

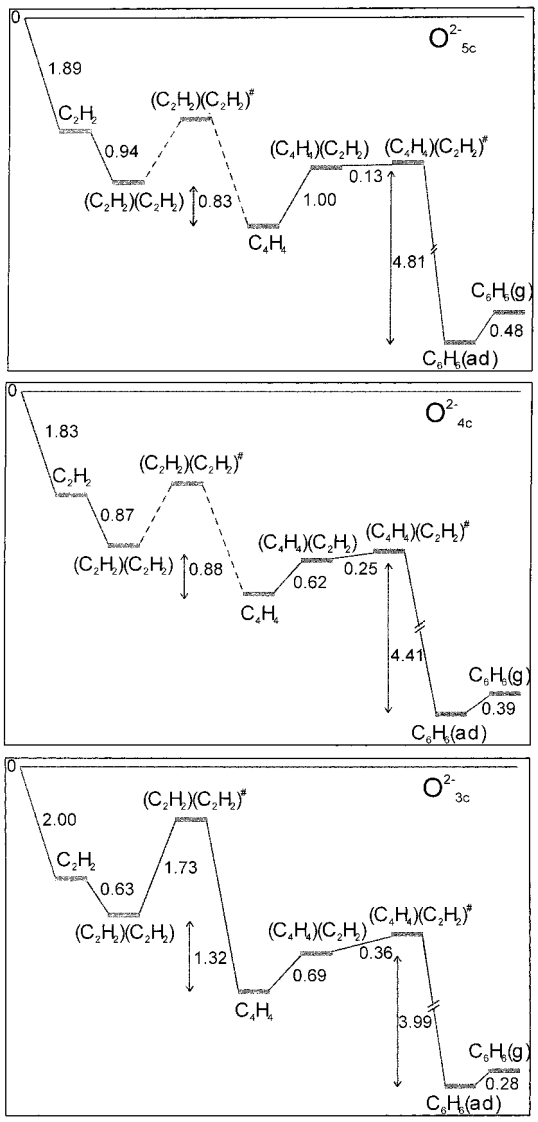

Figure 8. Reaction path for acetylene cyclization on Pd supported on a oxygen anion at terrace (O_{5C}^{2-}, top), edge (O_{4C}^{2-}, center), and corner (O_{3C}^{2-}, bottom) sites of the MgO surface. Energies (at the BP level) are in electronvolts. The transition state for the step $2C_2H_2 \rightarrow C_4H_4$ has not been identified for the case of O_{5C}^{2-} and O_{4C}^{2-} centers; the reaction path is indicated by a dotted line.

CpCo undergo acetylene trimerization via the cycloaddition mechanism;[17] second, the insertion reactions of olefins in metal−carbon σ bonds occur with high energy barriers.[46]

The cycloaddition process is activated and requires the overcoming of an energy barrier. The geometrical structure of the corresponding transition state, $Pd(C_4H_4)(C_2H_2)^{\ddagger}$, is rather different from the $Pd(C_4H_4)(C_2H_2)$ reactants as shown by the variation in the interfragment C−C distances, $d(C_{2-}C_3)$, Table 3. The transition energies are of 0.9−1.2 eV when the Pd atom is supported at F_{nC}^{+} centers located at terrace and edge sites, while it is higher, 1.5 eV, for the low-coordinated F_{3C}^{+} centers, Table 3 and Figures 3 and 7. As far as the neutral F_{nC} centers, only at the terrace sites the energy barrier, 0.8 eV, seems to be consistent with the observed reaction temperatures; on the contrary, supported Pd atoms at F_{4C} and F_{3C} centers give high activation energies (2 eV or more), Table 3 (but as we mentioned before, the relevance of these two sites is minimal since the adsorption of a single acetylene molecule hardly occurs).

At the oxide sites, O_{nC}^{2-}, the cycloaddition between $Pd(C_4H_4)$ and the coordinated acetylene is possible only by assuming a different mechanism, i.e., a direct attack of an acetylene molecule from the gas-phase without formation of the $Pd(C_4H_4)(C_2H_2)$ complex which is unstable or metastable, as discussed in the previous section. A similar mechanism has been proposed in the case of acetylene trimerization with phosphine substituted CpCo homogeneous catalyst.[17] We have verified that the approach of acetylene to the $Pd(C_4H_4)$ complex leads to a distortion of the C_4H_4 fragment from its equilibrium geometry and to a transition state with similar structure of the activated complex at BP and B3LYP levels. However, direct cycloaddition requires overcoming an energy barrier comparable to that implying acetylene coordination (the overall energetic cost is 1.05 eV at the BP level and 1.52 eV at the B3LYP level for the O_{3C}^{2-}).

Once formed, benzene promptly desorbs since it is unbound at neutral F_{nC} centers and only very slightly bound at the Pd/F_{nC}^{+} sites. This is at variance with Pd single crystals and Pd particles or clusters where benzene desorption is the rate-determining step. On the Pd_6 cluster model of Pd(111), Figure 5, the interaction of acetylene is considerably stronger than on single Pd atoms (the adsorption energy of a single acetylene is about 2 eV). The acetylene molecule is adsorbed on the hollow site as found in previous works.[1,7,47−49] Once the C_4H_4 intermediate is formed, the coordination of the third acetylene molecule is a favored process, with an energy gain of 0.9 eV. This stable structure, Figure 5C, results in a quite high barrier for the [4 + 2] addition, 1.5 eV. This transition state has been investigated to have a comparison with the supported Pd atom but is not necessarily the most favored one. The binding energy of benzene to Pd_6, about 2 eV, is larger than the barrier for cycloaddition, consistent with a desorption temperature of about 500 K and with the fact that on Pd(111) benzene desorption, and not the cycloaddition, is the rate-determining step.

4. Discussion and Conclusions

The overall $Pd + 3C_2H_2 \rightarrow Pd(C_6H_6)$ process on MgO thin films is thermodynamically very favored and includes two individual steps which imply overcoming an energy barrier. Our estimates of the activation barriers are carried out at 0 K. The thermal correction and the vibrational entropy at 300 K have been evaluated for the Pd/F_{5C} complex by employing the rigid oscillator−hindered rotator method,[50] but their contribution to the activation energies is of the order of 1%. However, the intrinsic limitations connected with the method and models employed for the calculations (including the choice of the exchange-correlation functional) suggests that our barriers may be affected by errors of the order of a few tenths of an electronvolt. It is worth noticing that the computed barriers for the $Pd(C_4H_4)(C_2H_2)^{\ddagger}$ transition state on F_S and F_S^{+} follow the linear relationship of Brønsted−Evans−Polanyi,[51,52] for the reaction occurring on terrace, edge, and corner. This empirical relation, which can be used to estimate activation barriers,[53] states that there is a linear relationship between the activation energy and the reaction energy, depending on the active site. This relation is not valid for the $Pd(C_2H_2)(C_2H_2)^{\ddagger}$ transition state, because of the different geometrical structures assumed by the two reacting molecules at corner sites.

Not all surface sites behave in the same way in the reaction. In particular, two steps are critical, the coordination of the first and of the third acetylene molecules. On very strong basic sites (F_{nC} centers) the electron density is considerably delocalized over the Pd atom: the interaction with the acetylene molecule is dominated by the Pauli repulsion. As a result, the first acetylene molecule is weakly bound at the less basic centers,

TABLE 3: Adsorption Properties of Three C_2H_2 Molecule on the S/Pd Complex (S = O^{2-}, F_S, F_S^+)

		Pd	Pd/$O^{2-}{}_{5C}$	Pd/$O^{2-}{}_{4C}$	Pd/$O^{2-}{}_{3C}$	Pd/F_{5C}	Pd/F_{4C}	Pd/F_{3C}	Pd/$F^+{}_{5C}$	Pd/$F^+{}_{4C}$	Pd/$F^+{}_{3C}$
$(C_4H_4)(C_2H_2)$	$d(C_1–C_1)$, Å	1.461	1.492	1.487	1.490	1.466	1.466	1.466	1.455	1.440	1.448
	$d(C_2–C_1)$, Å	1.351	1.348	1.351	1.355	1.364	1.359	1.369	1.361	1.373	1.372
	$d(C_2–Pd)$, Å	2.006	2.123	2.155	2.137	2.121	2.150	2.167	2.085	2.136	2.111
	$d(C_3–C_3)$, Å	1.215	1.293	1.287	1.299	1.307	1.309	1.311	1.255	1.267	1.270
	$d(C_2–C_3)$, Å	4.197	3.036	3.170	3.266	3.439	3.687	3.670	3.518	3.744	3.742
	$d(C_3–Pd)$, Å	2.662	2.059	2.064	2.057	2.083	2.091	2.081	2.224	2.164	2.177
	$\angle(H–C_3–C_3)$, deg	177.9	146.1	147.6	143.2	140.4	139.5	139.7	157.7	153.6	152.3
	BE_{BP},[a] eV	0.30 (0.25)	−1.00	−0.62	−0.69	1.17 (0.85)	2.03 (1.88)	2.43 (2.28)	0.73 (0.75)	1.13	1.20
$(C_4H_4)(C_2H_2)^‡$	$d(C_1–C_1)$, Å		1.480	1.472	1.473	1.448	1.431	1.429	1.428	1.417	1.419
	$d(C_2–C_1)$, Å		1.354	1.361	1.363	1.375	1.388	1.403	1.376	1.388	1.397
	$d(C_2–Pd)$, Å		2.153	2.164	1.186	2.139	2.151	2.147	2.108	2.129	2.112
	$d(C_3–C_3)$, Å		1.289	1.286	2.186	1.292	1.290	1.301	1.268	1.264	1.272
	$d(C_2–C_3)$, Å		2.474	2.416	2.414	2.365	2.334	2.297	2.300	2.285	2.305
	$d(C_3–Pd)$, Å		2.082	2.100	2.104	2.164	2.194	2.166	2.307	2.343	2.244
	$\angle(H–C_3–C_3)$, deg		148.5	149.2	148.3	146.5	146.4	143.1	152.6	153.5	150.6
	$\Delta E_{BP}^‡$,[b] eV		0.13	0.25	0.36	0.98 (1.22)	1.99 (2.21)	2.43 (2.73)	0.86	1.16	1.53
C_6H_6	$d(C–C)$, Å	1.419	1.413	1.411	1.411	unbound	unbound	unbound	1.409	1.411	1.417
	$d(C–Pd)$, Å	2.294	2.602	2.652	2.684	unbound	unbound	unbound	2.768	2.617	2.577
	BE_{BP},[c] eV	2.21	0.48	0.39	0.28	unbound	unbound	unbound	0.32	0.61	0.51
	ΔE_{BP},[d] eV	3.61	4.81	4.41	3.99	3.99	2.53	1.86	4.46	3.61	2.76

[a] Binding energy, BE, computed as BE = E[S/Pd/$(C_4H_4)(C_2H_2)$] − E[C_2H_2] − E[S/Pd]; in parenthesis B3LYP results. [b] $\Delta E^‡$ = E[S/Pd/$(C_4H_4)(C_2H_2)^‡$] − E[S/Pd/$(C_4H_4)(C_2H_2)$]; in parenthesis B3LYP results. [c] Binding energy, BE, computed as BE = E[S/Pd/C_6H_6] − E[C_6H_6] − E[S/Pd]. [d] Computed as $\Delta E = -E$[S/Pd/C_6H_6] − E[S/Pd/$(C_4H_4)(C_2H_2)$].

like the F centers at terraces, F_{5C}, while it is unbound at the more basic sites such as low-coordinated F centers, where more charge is delocalized over the 5s Pd orbital. Thus, low-coordinated F_{3C} and F_{4C} centers are not consistent with the proposed mechanism. On moderate basic sites (oxide anions, $O_{nC}{}^{2-}$) the π back-donation from Pd to C_2H_2 is the fundamental contribution to the binding energy and the acetylene molecule is more strongly bound the more basic is the site (corner > edge > terrace). $F_{nC}{}^+$ centers reveal properties which are somehow in the middle: a less basic character (only one electron in the cavity) and the positive electrostatic potential at the adsorption site determine a more favorable balance between Pauli repulsion and π donation; moreover, other interaction contributions, like polarization or σ donation from the hydrocarbon to Pd, have a nonnegligible role in the bonding. On these sites the first acetylene molecule binds easily.

In the presence of a preadsorbed hydrocarbon fragment the attack of another molecule is favored in the case of very basic sites such as the F centers. In fact, in this case the excess of electron density becomes an advantage for bonding. This is particularly important in the coordination of the third alkyne. In fact, this interaction is energetically favored only when the Pd atom is supported at *strong* basic sites, like the F_s and $F_s{}^+$ centers. On the contrary, oxide anions cannot provide to the metal enough electron density to simultaneously bind the intermediate species, C_4H_4, and the incoming alkyne molecule.

TDS experiments indicate that on MgO-supported Pd atoms benzene is exclusively produced at 300 K.[13,16] Using a preexponential factor of 10^{-13} s^{-1}, this corresponds to a rate determining step with a barrier of about 1 eV. Our calculations clearly show that benzene desorption is almost nonactivated and that the rate determining step is connected with the 2 + 2 and 4 + 2 cycloadditions via either the $Pd(C_2H_2)(C_2H_2)^‡$ or the $Pd(C_4H_4)(C_2H_2)^‡$ transition states. Among the F centers, only for F_{5C}, $F_{5C}{}^+$, and $F_{4C}{}^+$ sites the computed barriers are in the 1 eV range or lower, Figures 6 and 7. All other sites exhibit barriers which are incompatible with benzene formation at 300 K.

The combined thermodynamic and kinetic analysis of the process presented in this work indicates that cyclotrimerization of acetylene to form benzene *is possible only at Pd atoms supported at specific basic sites.* These sites are the terrace F_{5C} and the $F_{5C}{}^+$ centers (the present results suggest that also an O vacancy at an edge site, $F_{4C}{}^+$, is compatible with the reaction); this is completely consistent with the evidence that the Pd atoms are stabilized at these sites, as recently shown by a careful analysis of the properties of CO adsorbed on Pd_1/MgO.[18] In conclusion, the energetics of the trimerization reaction, together with our previous study of the CO adsorption properties,[18] provide strong compelling evidence of the critical role played by MgO oxygen vacancies not only in stabilizing the deposited metal atoms but also in determining the mechanism and the energetics of the chemical reactions occurring on these atoms.

Acknowledgment. This work is supported in part by the Italian INFM through the PRA-ISADORA project.

References and Notes

(1) Tysoe, W. T.; Nyberg, G. L.; Lambert, R. M. *J. Chem. Soc., Chem. Commun.* **1983**, 623−625.

(2) Sesselmann, W. S.; Woratschek, B.; Ertl, G.; Kuppers, J.; Haberland, H. *Surf. Sci.* **1983**, *130*, 245.

(3) Holmblad, P. M.; Rainer, D. R.; Goodman, D. W. *J. Phys. Chem. B* **1997**, *101*, 8883−8886.

(4) Abdelrehim, I. M.; Pelhos, K.; Madey, T. E.; Eng, J.; Chen, J. G. *J. Mol. Catal., A* **1998**, *131*, 107.

(5) Gentle, T. M.; Muetterties, E. L. *J. Phys. Chem.* **1983**, *87*, 2469−2472.

(6) Rucker, T. G.; Logan, M. A.; Gentle, T. M.; Muetterties, E. L.; Somorjai, G. A. *J. Phys. Chem.* **1986**, *90*, 2703−2708.

(7) Hoffmann, H.; Zaera, F.; Ormerod, R. M.; Lambert, R. M.; Yao, J. M.; Saldin, D. K.; Wang, L. P.; Bennett, D. W.; Tysoe, W. T. *Surf. Sci.* **1992**, *268*, 1.

(8) Patterson, C. H.; Lambert, R. M. *J. Am. Chem. Soc.* **1988**, *110*, 6871.

(9) Ormerod, R. M.; Lambert, R. M. *J. Phys. Chem.* **1992**, *96*, 8111−8116.

(10) Ormerod, R. M.; Lambert, R. M.; Hoffmann, H.; Zaera, F.; Yao, J. M.; Saldin, D. K.; Wang, L. P.; Bennet, D. W.; Tysoe, W. T. *Surf. Sci.* **1993**, *295*, 277.

(11) Pacchioni, G.; Lambert, R. M. *Surf. Sci.* **1994**, *304*, 208−222.

(12) Sanchez, A.; Abbet, S.; Heiz, U.; Schneider, W.-D.; Häkkinen, H.; Barnett, R. N.; Landmann, U. *J. Phys. Chem. A* **1999**, *103*, 9573.

(13) Abbet, S.; Sanchez, A.; Heiz, U.; Schneider, W.-D.; Ferrari, A. M.; Pacchioni, G.; Rösch, N. *J. Am. Chem. Soc.* **2000**, *122*, 3453.

(14) Abbet, S.; Sanchez, A.; Heiz, U.; Schneider, W.-D.; Ferrari, A. M.; Pacchioni, G.; Rösch, N. *Surf. Sci.* **2000**, *454/456*, 984.

(15) Abbet, S.; Sanchez, A.; Heiz, U.; Schneider, W.-D. *J. Catal.* **2001**, *198*, 122.

(16) Ferrari, A. M.; Giordano, L.; Rösch, N.; Heiz, U.; Abbet, S.; Sanchez, A.; Pacchioni G. *J. Phys. Chem.* **2000**, *104*, 10612

(17) Hardesty, J. H.; Koerner, J. B.; Albright, T. A.; Le, G. Y. *J. Am. Chem. Soc.* **1999**, *121*, 6055.
(18) Abbet, S.; Riedo, E.; Brune, H.; Heiz, U.; Ferrari, A. M.; Giordano, L.; Pacchioni, G. *J. Am. Chem. Soc.* **2001**, *123*, 6172.
(19) *Cluster Models for Surface and Bulk Phenomena*; Pacchioni, G., Bagus, P. S., Parmigiani, F., Eds.; NATO ASI Series B; Plenum Press: New York, 1992; Vol. 283.
(20) Nygren, M. A.; Pettersson, L. G. M.; Barandiaran, Z.; Seijo, L. *J. Chem. Phys.* **1994**, *100*, 2010.
(21) Ferrari, A. M.; Pacchioni, G. *Int. J. Quantum Chem.* **1996**, *58*, 241.
(22) Ferrari, A. M.; Soave, R.; D'Ercole, A.; Pisani, C.; Giamello, E.; Pacchioni, G. *Surf. Sci.* **2001**, *479*, 83.
(23) Ditchfield, R.; Hehre, W.; Pople, J. A. *J. Chem. Phys.* **1971**, *54*, 724.
(24) Soave, R.; Ferrari, A. M.; Pacchioni, G. *J. Phys. Chem. B* **2001**, *105*, 9798.
(25) Hay, P. J.; Wadt, W. R. *J. Chem. Phys.* **1985**, *82*, 299.
(26) Lopez, N.; Illas, *J. Phys. Chem.* **1998**, *102*, 1430.
(27) Lopez, N.; Illas, F.; Rösch, N.; Pacchioni, G. *J. Chem. Phys.* **1999**, *110*, 4873.
(28) Ranney, J. T.; Starr, D. E.; Musgrove, J. E.; Bald, D. J.; Campbell, C. T. *Faraday Discuss.* **1999**, *114*, 195.
(29) Becke, A. D. *Phys. Rev. A* **1988**, *38*, 3098.
(30) Perdew, J. P. *Phys. Rev. B* **1986**, *33*, 8822.
(31) Becke, A. D. *J. Chem. Phys.* **1993**, *98*, 5648.
(32) Lee, C.; Yang, W.; Parr, R. G. *Phys. Rev. B* **1988**, *37*, 785.
(33) Boys, S. F.; Bernardi, F. *Mol. Phys.* **1970**, *19*, 553.
(34) Frisch, M. J.; et al. *Gaussian98*; Gaussian Inc.: Pittsburgh, PA, 1998.
(35) Bagus, P. S.; Hermann, K.; Bauschlicher, C. W. *J. Chem. Phys.* **1984**, *80*, 4378.
(36) Bredow, T.; Marquez, A. M.; Pacchioni, G. *Surf. Sci.* **1999**, *430*, 137.
(37) Dupuis, M.; Johnston, F.; Marquez, A. *HONDO 8.5 for CHEM-Station*; IBM Co.: Kingston, NY, 1994.
(38) Matveev, A. V.; Neymann, K. M.; Yudanov, I. V.; Rösch, N. *Surf. Sci.* **1999**, *426*, 123.
(39) Giordano, L.; Goniakowski, J.; Pacchioni, G. *Phys. Rev. B* **2001**, *64*, 075417.
(40) Yudanov, I. V.; Vent, S.; Neyman, K.; Pacchioni, G.; Rösch, N. *Chem. Phys. Lett.* **1997**, *275*, 245.
(41) Goniakovski, J. *Phys. Rev. B* **1998**, *58*, 1189.
(42) Ferrari, A. M.; Pacchioni, G. *J. Phys. Chem.* **1996**, *100*, 9032.
(43) Abbet, S.; Heiz, U.; Häkkinen, H.; Landman, U. *Phys. Rev. Lett.* **2001**, *86*, 5950.
(44) Shustorovich, E. *Surf. Sci. Rep.* **1986**, *6*, 1.
(45) The geometry and binding energy of the $Pd(C_4H_4)$ intermediate are quite similar to those reported in a previous investigation.[16] Only in the case of $Pd/O^{2-}{}_{3C}$ and $Pd/O^{2-}{}_{4C}$ is the structure, almost perpendicular to the surface, different from that described in ref 16 (almost parallel to the substrate). This is because two minima exists for the same complex; the configuration shown in Figure 2D ("normal") is about 0.5 eV more stable than the metastable form reported in ref 16.
(46) Crabtree, R. H. *The Organometallic Chemistry of the Transition Elements*, 2nd ed.; Wiley: New York, 1994.
(47) Demuth, J. E. *Surf. Sci.* **1979**, *84*, 315.
(48) Gates, J. A.; Kesmodel, L. L. *Surf. Sci.* **1983**, *124*, 68.
(49) Timbrell, P. Y.; Gellman, A. J.; Lambert, R. M.; Willis, R. F. *Surf. Sci.* **1988**, *206*, 339.
(50) Sauer, J.; Ugliengo, P.; Garrone, E.; Saunders, V. R. *Chem. Rev.* **1994**, *94*, 2095.
(51) Brønsted, N. *Chem. Rev.* **1928**, *5*, 231.
(52) Evans, M. G.; Polanyi, N. P. *Trans. Faraday Soc.* **1938**, *34*, 11.
(53) Logarottir, A.; Rod, T. H.; Nørskov, J. K.; Hammer, B.; Dahl, S.; Jacobsen, C. J. H. *J. Catal.* **2001**, *197*, 229.